Influence of Cardiolipin on the Functionality of the Q_A Site of the Photosynthetic Bacterial Reaction Center

Mauro Giustini,[†] Francesco Castelli,[†] Ivan Husu,[†] Marcello Giomini,[†] Antonia Mallardi,[‡] and Gerardo Palazzo*[,§]

Dipartimento di Chimica, Università "La Sapienza", I-00185 Roma, Italy, Istituto per i Processi Chimico-Fisici, CNR, 70126 Bari, Italy, and Dipartimento di Chimica, Università di Bari, via Orabona 4, I-70126, Bari, Italy

Received: July 25, 2005; In Final Form: September 13, 2005

The effect of cardiolipin on the functionality of the Q_A site of a photosynthetic reaction center (RC) was studied in RCs from the purple non-sulfur bacterium *Rhodobacter sphaeroides* by means of time-resolved absorbance measurements. The binding of the ubiquinone-10 to the Q_A site of the RC embedded in cardiolipin or lecithin liposomes has been followed at different temperatures and phospholipid loading. A global fit of the experimental data allowed us to get quite reliable values of the thermodynamic parameters joined to the binding process. The presence of cardiolipin does not affect the affinity of the Q_A site for ubiquinone but has a marked influence on the rate of $P^+Q_A^- \rightarrow PQ_A$ electron transfer. The $P^+Q_A^-$ charge recombination kinetics has been examined in liposomes made of cardiolipin/lecithin mixtures and in detergent (DDAO) micelles doped with cardiolipin. The electron-transfer rate constant increases upon cardiolipin loading. It appears that the main effect of cardiolipin on the electron transfer can be ascribed to a destabilization of the charge-separated state. Results obtained in micelles and vesicles follow the same titration curve when cardiolipin concentration evaluated with respect to the apolar phase is used as a relevant variable. The dependence of the $P^+Q_A^-$ recombination rate on cardiolipin loading suggests two classes of binding sites. In addition to a high-affinity site (compatible with previous crystallographic studies), a cooperative binding, involving about four cardiolipin molecules, takes place at high cardiolipin loading.

1. Introduction

Proteins perform an astonishing variety of functions and roles. Actually, almost all the processes taking place in a living organism (e.g., signal transmission, muscle contraction, photosynthesis, respiration, immune response) can be pictured out merely in terms of protein functions (the transmission of genetic information is the notable exception). Only when further insight is required does one have to take carefully into account the role of membranes, ions, and so on. For this pivotal role in the biological realm, the structure and the function of proteins have been extensively studied. Often the structural information gives a solid ground to understanding protein functionality (e.g., the celebrated Pauling's description of the sickle-cell anemia as a *molecular disease*).[1] Unfortunately, to obtain a high-resolution structure in the case of integral membrane proteins is much more difficult than water-soluble proteins.[2] Among the best determined structures of a polytopic membrane protein are the bacterial photosynthetic reaction centers (RCs), which were the first integral membrane proteins to yield high-resolution X-ray structures. About two decades ago, structures were determined for RCs from two species of purple bacteria (*Blastochloris viridis*[3] and *Rhodobacter* (*Rb.*) *sphaeroides*[4]). The RC is an integral pigment−protein complex spanning the intracytoplasmic membrane of photosynthetic bacteria and promoting light-induced charge separation across the membrane dielectric.[5] It can be extracted from bacterial membranes by using suitable detergents, for example, *N*,*N*,-dimethyldodecylamine-*N*-oxide (DDAO). According to X-ray diffraction studies, the RC from *Rb. Sphaeroides* consists of three polypeptides, named L, M, and H. The L and M subunits bind noncovalently nine cofactors in twofold symmetric branches: four bacteriochlorophyll molecules, two bacteriopheophytins, two ubiquinones (Q_A and Q_B), and a non-heme iron Fe^{2+}.[6] The protein scaffolding holds the various cofactors in their appropriate position for an efficient electron transfer. Two of the bacteriochlorophyll molecules, located on the periplasmic side of the membrane, are organized as an excitonic dimer acting as the primary photoinduced electron donor (P).[5,6] The charge separation involves the transfer of an electron from P to the primary ubiquinone acceptor (Q_A). Electron transfer normally proceeds from Q_A^- to the secondary ubiquinone (Q_B).[7] In the absence of any exogenous electron donor to P^+ (e.g., in solutions of purified protein), the light-induced electron transfer from P to the acceptor quinone complex (Q_A or Q_B) is followed by the dark reduction of P^+ (reflecting the charge recombination from reduced acceptor quinones).[8]

Because of continuous improvement in the resolution and quality of crystallographic structures of the wild-type and of a plethora of mutants, the bacterial RC is still playing the role of the archetype in the study of general principles of membrane protein architecture and dynamics and of biological electron transfer.[9,10] An interesting consequence of the increased quality of X-ray diffraction data was the safe attribution of large regions of electron density to given molecules of bound phospholipid.[11−13] Generally speaking, this is of considerable interest, as a huge

* To whom correspondence should be addressd. Address: Dipartimento di Chimica, via Orabona 4, I-70126, Bari, Italy. E-mail: palazzo@chimica.uniba.it.

[†] Università "La Sapienza".

[‡] Istituto per i Processi Chimico-Fisici.

[§] Università di Bari.

10.1021/jp054104d CCC: $30.25
Published on Web 10/14/2005

amount of functional studies has revealed the great importance of protein−lipid interactions for the function of membrane proteins.[14,15] Quite peculiarly, in the case of bacterial RC, evidences of a specific role of phospholipids in the RC reactivity are still very poor, being limited to three recent papers concerning some effects of cardiolipin (bis-phosphatidylglycerol) on the functionality of the Q_B site[16,17] and on the thermal stability of the protein.[18] On the contrary, the presence of a binding site for a cardiolipin molecule was assessed by several crystallographic studies performed on both wild-type and mutant RCs crystallized *in surfo*[11−13,19] and *in cubo*.[20] In addition, the size, shape, and charge density of the pocket, which provide the binding site for a single cardiolipin molecule found in crystallographic studies are well preserved over a wide range of photosynthetic bacteria.[21] In the attempt to fill the gap between the numerous structural studies and the limited functional evidences, we have focused our attention on the influence that cardiolipin molecules exploit on the quinone binding to the Q_A site and on the $P^+Q_A^- \rightarrow PQ_A$ electron transfer. In the present work, the effect of cardiolipin on the functionality of the Q_A site was studied in RC-containing liposomes made of cardiolipin or lecithin as well as on RC-DDAO micelles.

2. Experimental Section

Cardiolipin (bis-phosphatidylglycerol), purified from bovine heart, was from Sigma in the form of lyophilized sodium salt, while terbutryne and dodecyl dimethylamine oxide (DDAO) were from Fluka. Soybean lecithin (1,2-diacyl-*sn*-glycero-3-phosphocholine) was a generous gift from Degussa Bioactives AG (brand Epikuron 200). All the chemicals have been used without further purification.

RCs from *Rb. Sphaeroides* were isolated and purified according to Gray et al.[22] In all the preparations, the ratio between the absorption at 280 nm and the absorption at 800 nm was about 1.2. Quinone-depleted RCs were prepared according to the method of Okamura et al.[23] All the quinone was removed from the Q_B site while approximately 60% of the RCs had been depleted of quinone at the Q_A site. The degree of occupancy of the Q_A site has been evaluated by comparing, in micelles, the extent of the flash-induced absorbance changes before and after the addition of a saturating concentration of the water soluble 2,3-dimethoxy-5-methyl-1,4-benzoquinone (from SIGMA).

The RC-containing vesicles (proteoliposomes) were prepared as follows. Phosphatidylcholine (PC) and/or cardiolipin (CL) were dissolved in chloroform, dried under N_2 flow, and resuspended in 10 mM imidazole, 100 mM KCl, and 3% Na-cholate buffer (pH = 7.0). RCs (in 10 mM Tris-HCl, 0.025% DDAO, pH = 8.0) were added to this suspension, previously sonicated until clarity. Detergent removal was obtained by eluting this suspension through a Sephadex G-50 (Pharmacia) column with 10 mM imidazole/100 mM KCl (pH = 7.0) buffer. Detergent removal results in RC-containing small unilamellar vesicles.[24]

Light-induced redox changes of the primary donor of the RC were monitored by a home-built kinetic single beam spectrophotometer realized with orthogonal geometry between measuring and exciting beams. The measuring beam was provided by a laser diode (Roithner Lasertechnik, $\lambda = 870$ nm), operating at an average power of 2 mW, illuminating the sample cuvette through a 0.5 mm diameter pinhole. A silicon photodiode (UDT, 10 D), working in photovoltaic mode in connection with a high-speed di-fet operational amplifier (Texas Intruments, OPA637AP), has been used as a detector (the time constant of the whole circuitry was kept to few microseconds). To avoid any interference from the exciting light, the measuring beam passed through a red glass filter (Corning, no. 2-64) placed in front of the 800 μm entry slit of a grating monochromator (Oriel, model 7240) between the sample and the detector. The exciting pulse was provided by a frequency doubled Nd:YAG laser (Quanta System, Handy 710, $\lambda = 532$ nm, 7 ns pulse width, 300 mJ/pulse). Data have been acquired by means of a 200 kS/s, 16-bit resolution acquisition card (National Instruments, PCI-6013 equipped with the BNC-2120 board) installed onto a PIII computer. The acquisition of the data was driven by home-built acquisition software developed in the LabView 6.0 environment. The acquisition software took care of the gating of the measuring light (turned on 5 s before starting each experiment and off immediately after the acquisition), the triggering of the exciting laser, the delay time among consecutive experiments, the number of data points (generally 4000), and the acquisition time. Typically, 8−12 scans (depending on RC concentration) were averaged in each experiment to have a S/N ratio of at least 20. The RC was left dark adapt between scans for at least 60 s. The temperature of the cell holder was kept constant (±0.2 K) using a thermocryostat (Julabo, model ED). The sample temperature was monitored by a Pt-100 ceramic resistor (Degussa, accuracy ±0.2 K) immersed directly into the cuvette and connected to a digital thermometer (Italmec, model VMD1).

In detergent solution, quinone-depleted RCs have shown only single-exponential $P^+Q_A^-$ recombination. At variance, when the same RCs are inserted in liposomes, a small fraction of proteins undergoing $P^+Q_B^-$ charge recombination is detected, and the overall P^+ decay can be accounted for by two exponentials. This is due to the statistical distribution of quinones and RCs among vesicles as described in ref 25. The addition of terbutryn (a competitive inhibitor for the Q_B site) restores the single-exponential $P^+Q_A^-$ decay. The amplitude of the bleaching at time $t = 0$ and the rate of $P^+Q_A^-$ recombination were found to be unaffected by the presence of the inhibitor.

Experimental data were fitted to the relevant equations by a least-squares routine based on the Simplex[26,27] algorithm implemented in the STEFIT software (Stelar snc). Given the cross-correlation between some best-fit parameters (see next section), the error associated with the *i*th fitting parameter was evaluated by means of Monte Carlo simulation as previously described.[28] In the calculation of local concentrations, we have used the following quantities: molecular volume of the lecithin hydrophobic tails[29] $v_{PC} = 1.053$ nm^3, molecular volume of the cardiolipin hydrophobic tails $v_{CL} = 2v_{PC}$, and DDAO molar volume[30] = 0.2557 L mol^{-1}.

3. Results

3.1. Quinone Binding. We have probed the kinetics of P^+ decay in *Rb. Sphaeroides* RCs reconstituted into liposomes and micelles by following flash-induced absorbance changes (ΔAbs) recorded at 870 nm (a representative trace is shown in the Appendix, Figure 6).

In the case of quinone-depleted RC, the charge separation is limited to the bacteriopheophytin molecule (the intermediate electron acceptor) and the subsequent charge recombination occurs on a sub-microsecond time scale. Therefore, with our experimental setup, it is not possible to detect any absorbance change. In the presence of a pool of quinone molecules, the binding sites of the protein are occupied by quinones according to

$$[RCQ_i] = \frac{[RC][Q]_f}{K_{D,Qi}} \quad (1)$$

where $[RCQ_i]$ indicates the protein concentration with the Q_i site occupied, K_{D,Q_i} is the dissociation constant for the *i*-site, and $[Q]_f$ and [RC] denote the free quinone and RC concentration, respectively. Since both the $P^+Q_A^-$ and the $P^+Q_AQ_B^-$ states are long-lived, in the presence of quinone, it is possible to follow the time course of the charge recombination. Furthermore, since the photoinduced electron transfer up to Q_B is possible only through Q_A, the proteins with the Q_B site occupied and the Q_A site empty do not contribute to the observed signal. The decay of P^+ following a light flash was monitored at 870 nm at different quinone concentrations ([Q]) and temperatures. The experimental traces were fitted to one or two exponentials (depending on their features) thus obtaining the amplitude of the bleaching at time $t = 0$. Such a quantity, $\Delta Abs(0)$, is proportional to the concentration of RC with the Q_A site occupied according to

$$\Delta Abs(0) = Z[RCQ_A] \tag{2}$$

where *Z* depends on the differences in the molar absorptivities between P^+ and P and on the degree of saturation of the light pulse. The contribution of the binding to the Q_B site can be neglected in the calculation of $[Q]_f$. Accordingly, for an isothermal binding curve, the following relationship holds

$$[RCQ_A] = \frac{([RC]_{tot} - [RCQ_A])([Q] - [RCQ_A])}{K_{D,Q_A}} \tag{3}$$

In the above equation $[RC]_{tot}$ denotes the total RC concentration ($[RC]_{tot} = [RC] + [RCQ_A]$). On this basis, the temperature dependence of quinone binding to RC can be described by taking into account the classical Van't Hoff relationship

$$K_{D,Q_A} = \exp\left(\frac{\Delta H^\circ}{RT} - \frac{\Delta S^\circ}{R}\right) \tag{4}$$

where *R* is the gas constant, *T* is the thermodynamic temperature, and ΔH° and ΔS° are the standard enthalpy and entropy changes associated to the quinone binding at the Q_A site.

The above description implicitly assumes that the binding interaction between RCs and quinone molecules occurs in a homogeneous system. Experimentally, such a situation is met in reverse micelles[31,28] or, when dealing with highly hydrophilic quinones, in aqueous dispersion of direct micelles.[32] Proteoliposomes are more complicated: they are microheterogeneous systems composed of an ensemble of disconnected hydrophobic domains where both RCs and quinones are inserted and statistically distributed, resulting in two additional complications. First, the quinone binding should be handled in terms of the relevant distribution functions. For most purposes, however, eqs 1−3 well describe the binding process in vesicles as long as one uses concentration (of quinone and RC) evaluated with respect to the apolar volume only[33] (for details see ref 34).

The second point is the tuning of quinone concentration in vesicles. It is very difficult to modulate with accuracy the concentration of ubiquinone within the bilayers.[35] This is a crucial point when dealing with the high-affinity Q_A site because one has to probe very low concentrations and the contribution of tightly bound quinone molecules cannot be neglected[36] (~40% of RC have the Q_A site still occupied in our preparations). It is clear that, under these constraints, the determination of binding isotherms is not feasible.

To overcome this problem, the binding at the Q_A site was studied at constant quinone concentration by varying the temperature. Light-induced absorbance changes were measured at different temperatures on the same sample. The proteoliposomes solution was first equilibrated at high temperature (~308 K) in the dark for 30 min and then cooled by steps of 4 K. At each temperature, the sample was incubated in the dark for 15′ before the measurement. At the end of the T-scan, the solution was warmed to 298 K to check for thermal hysteresis (differences are below 5%). Typical curves, $\Delta Abs(0)$ vs *T*, are shown in Figure 1 for proteoliposomes made of cardiolipin (panel A) and lecithin (panel B). For both the phospholipids the overall trend follows the dependence of K_{D,Q_A} on temperature observed in reverse micelles. That is, the lower the temperature, the tighter the binding, thus resulting in an increase in $\Delta Abs(0)$. In these experiments, the number of quinone molecules is fixed by the number of RCs and by the degree of occupancy of the Q_A site (40%). However, we have still some (limited) degrees of freedom in tuning the local quinone concentration by changing the phospholipid loading and thus the volume of the hydrophobic domains. As an example in Figure 1, data are shown that are collected at different phospholipid concentrations (reported as mg/mL, for all the samples, the overall RC concentration was 2.3 μM). A lower phospholipid loading results in a weaker *T* dependence. This is because at high quinone concentration (low phospholipid amount), the Q_A site is almost fully saturated, independent of the temperature. It should be stressed that one cannot compare $\Delta Abs(0)$ of different samples because the parameter *Z* in eq 2 depends on the degree of the light-pulse saturation and thus also on the scattering efficiency of liposome solutions. Actually, the $\Delta Abs(0)$ values tend to the same value at low temperature, and the curves of Figure 1 have been arbitrarily shifted for the sake of clarity.

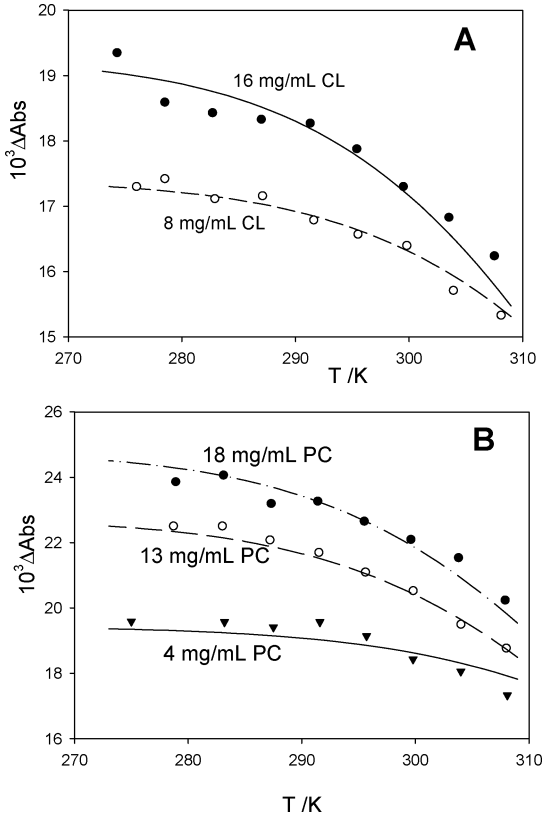

Figure 1. Q_A site functionality as a function of the temperature for the RC reconstituted in vesicles made of cardiolipin (panel A) and lecithin (panel B). Conditions: overall RC concentration = 2.3 μM, quinone/RC = 0.4. The curves are the global best-fit according to eqs 1−3 and 6 (the values of $\Delta G^\circ(T_{hm})$ and ΔH° are listed in Table 1). For the sake of readability the curves have been shifted vertically by adding a constant term.

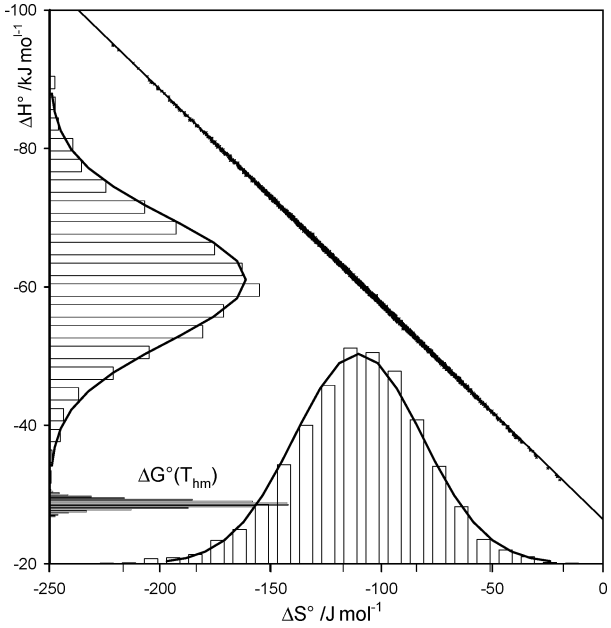

Figure 2. Monte Carlo (MC) analysis of quinone binding to the Q_A site in CL vesicles. The simultaneous fit of data in Figure 1, panel A, was analyzed by means of MC simulation as described in the text. The main graph shows the correlation plot $\Delta H°$ vs $\Delta S°$. It is evident that all the data follow a straight line with a correlation coefficient $r^2 = 0.9997$. The slope coincides to the mean harmonic temperature $T_{hm} = (1/n \sum_j^n 1/T_j)^{-1}$, with n being the number of experimental points; the intercept corresponds to the standard free energy of binding at T_{hm}. Histograms (open bars) representing the frequency of $\Delta H°$ and $\Delta S°$ are drawn on the ordinate and abscissa, respectively. The frequency for $\Delta G°(T_{hm})$ according to eq 6 is also drawn on the ordinate. Due to the large statistical enthalpy−entropy compensation, large spreads of $\Delta H°$ and $\Delta S°$ result in a moderate uncertainty on $\Delta G°(T_{hm})$. Analysis of quinone binding in PC vesicles (i.e., data of Figure 1, panel B) furnishes essentially the same results.

It appears that the RC in vesicles made of both CL and PC follows qualitatively the predictions of eqs 1−4. For a given phospholipid, it is possible to fit simultaneously all the data sets to eqs 1−4. In such a global analysis[37] for each sample, [Q] is a known quantity and Z an adjustable parameter. Of course all the samples share the same $\Delta H°$ and $\Delta S°$.

Unfortunately $\Delta H°$ and $\Delta S°$ are strongly correlated in the Van't Hoff relation (eq 4) and the independent variables (T and [Q]) can be tuned only on limited ranges. Monte Carlo (MC) simulation furnishes a straightforward evaluation of the significance of the values calculated under these conditions.[38,39] The distribution of $\Delta H°$ and $\Delta S°$ obtained from Monte Carlo analysis of the data (1000 runs in each case) is shown in Figure 2 in the case of CL vesicles, and it clearly illustrates the large uncertainties associated with the best-fit parameters. The evident strong statistical correlation between enthalpy and entropy is the usual compensation between regression parameter estimates that occurs because the range of variation of the independent variable (T^{-1}) is small. Consequently, the correlation is linear with a slope near the harmonic mean temperature $T_{hm}=\langle 1/T\rangle^{-1}$ as predicted already 30 years ago by Krug and co-workers.[40] As shown in Figure 2, $\Delta H°$ follows the equation of a straight line if reported as a function of $\Delta S°$. It was demonstrated that the slope of such a line is equal to the mean harmonic temperature and the intercept is a measure of the free energy change at T_{hm} (hereafter $\Delta G°(T_{hm})$).[40] In formulas

$$\Delta H° = \Delta G°(T_{hm}) + T_{hm}\Delta S° \qquad (5)$$

Using the above relation, one can easily rewrite eq 4 as

$$K_{D,Q_A} = \exp\left(\frac{\Delta G°(T_{hm}) - \Delta H°}{RT_{hm}} + \frac{\Delta H°}{RT}\right) \qquad (6)$$

By means of such a transformation, we can describe the dependence of binding equilibrium on temperature in terms of two parameters ($(\Delta G°(T_{hm})$ and $\Delta H°$) whose estimates are statistically independent of one another.[40] It is therefore possible to fit the experimental data to eqs 1−3 and 6 and to quantify the affinity of the quinone for the primary acceptor binding site through the free energy change at $T_{hm} = 291$. Equations 1−3 and 6 nicely describe the experimental data (see curves in Figure 1). The best-fit parameters obtained by means of the above-described procedure (listed in Table 1) were independent of the class of phospholipid used. The quinone affinity for the Q_A site of RC is higher in vesicles than that previously found in reverse micelles (third column in Table 1). A similar result was found for the binding of quinone at the Q_B site.[34] According to Table 1, the main difference in quinone binding between vesicles and reverse micelles is due to the entropic contribution. Actually, the entropy cost to be paid upon binding is $\Delta S° = -180$ J/mol in reverse micelles but only about -110 J/mol in vesicles. Likely this is due to the fact that the degrees of freedom associated with the unbound quinone are less in the bilayer (a crowded bidimensional environment) than in the large organic bulk surrounding the reverse micelles.

More importantly, the quinone affinity at 291 K is the same for cardiolipin and lecithin (within 3%), and also, the enthalpy and entropy changes determined in both CL and PC liposomes seem to be essentially the same. On these bases, it seems that the presence of a high concentration of cardiolipin does not induce gross changes in the interactions taking place between the ubiquinone molecules and the protein within the Q_A binding site. On the contrary, cardiolipin strongly affects the rate of charge recombination between P^+ and Q_A^- as detailed in the following section.

3.2. $P^+Q_A^- \rightarrow PQ_A$ Electron Transfer. The photoinduced charge separation and the subsequent charge recombination for RCs with only the Q_A site occupied are described by[6]

$$PQ_A \underset{k_{AP}}{\overset{h\nu}{\rightleftharpoons}} P^+ Q_A^- \qquad (7)$$

These electron-transfer processes, being intramolecular, obey first-order kinetics (see, however, refs 41 and 42). The temperature dependence of $P^+Q_A^-$ recombination kinetics has been examined in liposomes made of PC and CL and in detergent micelles as well. The main results are presented in Figure 3. The charge recombination rate constants (k_{AP}), observed in different environments, are of the same order of magnitude and speed up when cooling as recognized by several authors in previous studies on detergent micelles.[41,43−46] However, k_{AP} values obtained in proteoliposomes made of different phospholipids are clearly different. At all the temperatures, the charge recombination kinetics in CL proteoliposomes are systematically faster than those observed in PC proteoliposomes. For the purpose of comparison in Figure 3, the results obtained in RC

TABLE 1: Thermodynamical Parameters for the Ubiquinone Binding to the Q_A Site of RC[a]

	CL vesicles	PC vesicles	reverse micelles[b]
$\Delta G°(T_{hm})$/kJ mol^{-1}	-29 ± 1	-28 ± 1	-22.3 ± 0.1
$\Delta H°$/kJ mol^{-1}	-60 ± 10	-70 ± 15	-75 ± 3
$\Delta S°$/J mol^{-1}	-110 ± 30	-120 ± 30	-180 ± 10

[a] The reference state is 1 M with respect to the apolar volume, $T_{hm} = 291$ K. [b] From ref 28.

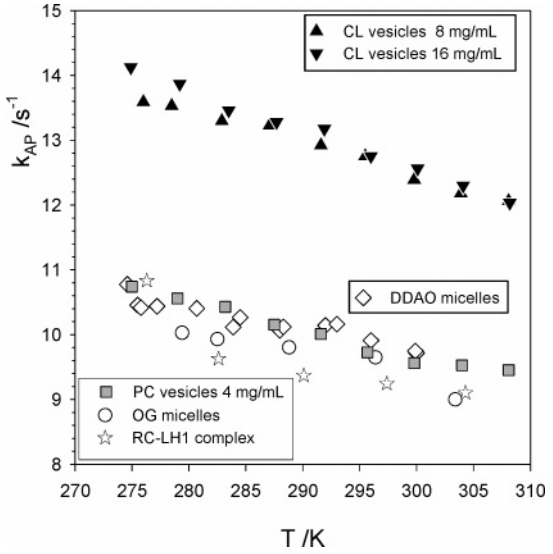

Figure 3. Rate constant of $P^+Q_A^-$ recombination as a function of temperature for reaction centers in different systems: CL vesicles (closed triangles), PC vesicles (gray squares), detergent micelles (open symbols), and core complex (stars). Data in micelles of octylglucoside (OG) and core complex (RC-LH1) are from ref 47; for other assays, the RC concentration was 2.3 μM.

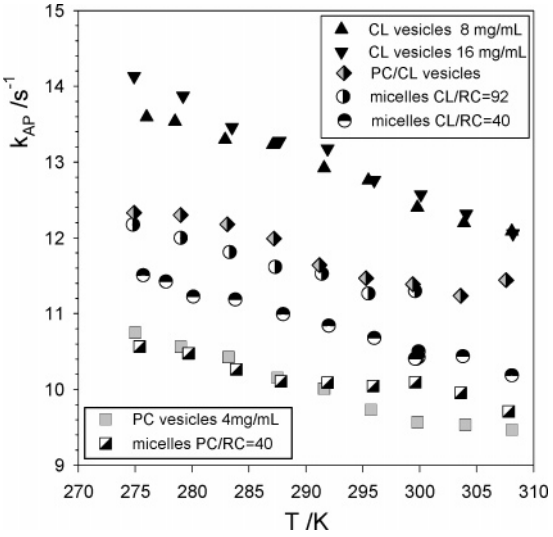

Figure 4. Rate constant of $P^+Q_A^-$ recombination as a function of temperature for reaction centers solubilized in DDAO micelles doped with different amounts of CL (semi-filled circles). Also shown are the results found for DDAO micelles doped with PC (semi-filled squares) and for vesicles made of a mixture of CL and PC (50 mol % in CL, 15 mg/mL of total lipids (semi-filled diamonds)). In the case of micelles, CL or PC loading is expressed as a lipid/RC mole ratio. For the purpose of comparison, data are shown for vesicles made of pure CL and PC (same symbols as in Figure 3).

suspended in DDAO and octylglucoside (OG) micelles and in core complexes are also reported[47] (the light-harvesting antenna complex, LH1, shows a circular arrangement that allows the LH1 to locate inside the RC, forming the so-called core complex).[48]

Quite surprisingly, CL vesicles represent the notable exception of a general trend. Figure 3 shows that PC vesicles, direct micelles made of two different detergents, and core complexes share essentially the same behavior with respect to the backward electron transfer. This finding suggests that the increase (30%) in the rate of $P^+Q_A^-$ recombination observed for RC embedded in CL vesicles is unrelated to the physical assembly of RC within the bilayer but is likely dependent on the binding of cardiolipin molecules to the protein. Accordingly, the investigation was extended to the RC solubilized in detergent (DDAO) micelles loaded with cardiolipin (Figure 4). For all the tested temperatures, k_{AP} increases upon CL loading. On the contrary, the addition of lecithin to the RC in DDAO solution does not change the rate of charge recombination. Interestingly, the k_{AP} value for RCs embedded in liposomes made of both the phospholipids (CL 50 mol %) is lower than that measured in liposomes made of pure CL. As a whole, the results of Figure 4 strengthen the hypothesis of some specific interaction (binding) between cardiolipin and the RC. This point was further afforded in the case of the RC solubilized by DDAO micelles. In such a system, the ratio CL/RC is easily tuned by adding cardiolipin as a concentrated alcoholic solution.[16] The results of this isothermal ($T = 299$ K) titration are shown in Figure 5. For the purpose of comparison, in the same figure, the relevant data of Figure 4 are also shown. The ordinate of Figure 5 represents the ratio k_{AP}/k_{AP}^0, with k_{AP}^0 being the rate constant observed in DDAO without cardiolipin. The abscissa of Figure 5 represents the cardiolipin concentration evaluated with respect to the apolar volume of the aggregates. This choice should be the relevant parameter for the binding process (because RC and CL are both water insoluble) and permits a consistent treatment of data collected in micelles and liposomes. The cardiolipin concentration in the apolar phase was evaluated according to

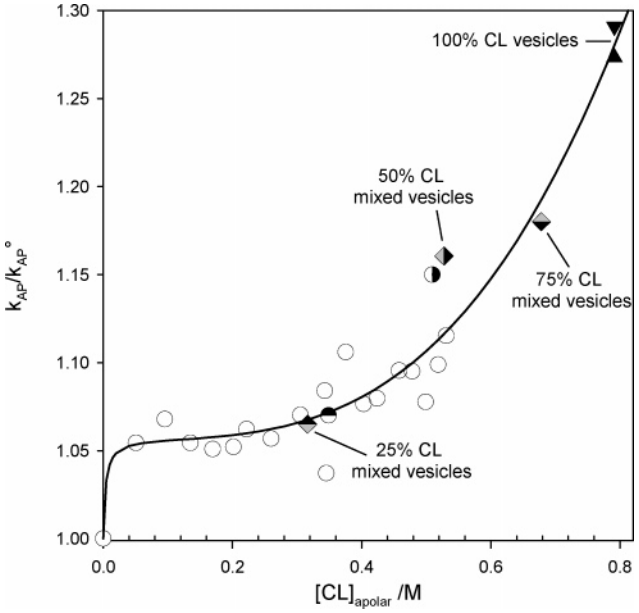

Figure 5. Isothermal ($T = 299$ K) CL titration of RC. The abscissa is the cardiolipin concentration evaluated with respect to the apolar volume (eq 8); the ordinate is the rate constant of $P^+Q_A^-$ recombination normalized to the rate found in DDAO micelles ($[CL]_{apolar} = 0$). The circles denote experiments in micelles (the two semi-filled circles are from Figure 4). The results obtained in liposomes made of pure CL (closed triangles) and of CL−PC mixtures (semi-filled diamonds) are also shown (the vesicles composition is expressed as CL mol %). The solid curve is the best-fit of the data to eq 17; best-fit parameters are $Y^1 = 1.06 \pm 0.02$, $Y^* = 6 \pm 2$, $n = 4 \pm 1$, $K^1 = 4 \pm 3$ mM, and $K_0 = (K^*)^{1/n} = 0.46 \pm 0.07$ M.

$$[\mathrm{CL}]_{\mathrm{apolar}} = \frac{n_{\mathrm{CL}}}{n_{\mathrm{CL}}\upsilon_{\mathrm{CL}} + n_{\mathrm{A}}\upsilon_{\mathrm{A}}} \qquad (8)$$

where n_{CL} = moles of cardiolipin, n_A = moles of the other amphiphile (PC or DDAO), and υ_{CL} and υ_A are the molar volumes of cardiolipin and amphiphile evaluated by taking into

account only the apolar moiety (tail). In the case of DDAO, n_A was evaluated by assuming 250 DDAO molecules per RC.[49]

As a whole, the data presented in Figure 5 suggest a mechanism of binding of CL to RC substantially independent of the system where the interaction has been evaluated. It has to be noted, in fact, that the experimental points of Figure 5 refer to samples of different nature: RC in DDAO micelles (at different ethanol content), RC in pure CL vesicles, and RC in mixed PC/CL vesicles. The presence of a trace amount of CL induces a small (5%) but highly reproducible jump in the k_{AP}/k_{AP}^0 value (remember that in the absence of added cardiolipin k_{AP}^0 is the same for RCs in different environments, Figures 3 and 4). The rate constant of $P^+Q_A^-$ decay remains almost unchanged upon CL loading until a sudden increase in the k_{AP}/k_{AP}^0 value is observed for $[CL]_{apolar} \sim 0.5$ M. Assuming that the binding of cardiolipin influences somehow the rate of electron transfer between Q_A^- and P^+, the evolution of the quantity k_{AP}/k_{AP}^0 upon CL loading suggests the existence of two classes of binding sites for CL, as found in the case of bovine heart cytochrome oxidase.[50] Thus, we have tentatively described the P^+ decay following the flash-induced charge separation according to scheme 9.

$$\begin{array}{ccc} P^+Q_A^- \cdot CL & \xrightarrow{k_{AP}^1} & PQ_A \cdot CL \\ K^1 \quad \updownarrow & & \\ P^+Q_A^- & \xrightarrow{k_{AP}^o} & PQ_A \\ K^* \quad \updownarrow & & \\ P^+Q_A^- \cdot (CL)_n & \xrightarrow{k_{AP}^*} & PQ_A \cdot (CL)_n \end{array} \qquad (9)$$

$P^+Q_A^-$ represents the charge-separate state of native RC, while $P^+Q_A^-\cdot$CL and $P^+Q_A^-\cdot(CL)_n$ represent RCs with cardiolipin molecules bound to two different classes of binding sites. K^1 is the dissociation constant for the first binding site

$$K^1 = \frac{[P^+Q_A^-][CL]}{[P^+Q_A^-\cdot CL]} \qquad (10)$$

while K^* describes the cooperative binding of cardiolipin to the RC according to the Hill equation

$$K^* = K_0^n = \frac{[P^+Q_A^-][CL]^n}{[P^+Q_A^-\cdot (CL)_n]} \qquad (11)$$

In the above equation, K_0 is the dissociation constant of the elementary step of the cooperative process. According to scheme 9, the different RC−CL complexes relax to the neutral state with different rate constants, namely, k_{AP}^0, k_{AP}^1, and k_{AP}^*. The time course of the observed P^+ decay depends on the rates of the CL binding/release and charge recombination processes. In the following, we will assume that the CL exchange is fast compared to the charge recombination (the result does not change in case of slow exchange as discussed in the Appendix).

Assuming a fast exchange, the rate of decay of the radical cation P^+ after the light pulse is

$$\frac{d[P^+]}{dt} = -k_{AP}^0[P^+Q_A^-] - k_{AP}^1[P^+Q_A^-\cdot CL] - k_{AP}^*[P^+Q_A^-\cdot (CL)_n] \qquad (12)$$

where $[P^+]$ is the concentration of all the charge separated states ($[P^+] = [P^+Q_A^-] + [P^+Q_A^-\cdot CL] + [P^+Q_A^-\cdot (CL)_n]$). Introducing the fractions $\alpha = [P^+Q_A^-\cdot CL]/[P^+]$ and $\beta = [P^+Q_A^-\cdot (CL)_n]/[P^+]$, eq 12 can be rewritten as

$$\frac{d[P^+]}{dt} = -\{k_{AP}^0(1-\alpha-\beta) + k_{AP}^1\alpha + k_{AP}^*\beta\}[P^+] \qquad (13)$$

In other words, assuming a fast exchange, scheme 9 predicts still a single-exponential decay of P^+ with an observed rate constant k_{AP} given by eq 14

$$k_{AP} = k_{AP}^0(1-\alpha-\beta) + k_{AP}^1\alpha + k_{AP}^*\beta \qquad (14)$$

Since eqs 10 and 11 can be rewritten in terms of α and β

$$K^1 = \frac{(1-\alpha-\beta)[CL]}{\alpha}$$

$$K^* = \frac{(1-\alpha-\beta)[CL]^n}{\beta} \qquad (15)$$

the experimentally observed k_{AP} depends on the binding equilibria according to

$$k_{AP} = \frac{k_{AP}^0K^1K^* + k_{AP}^1K^*[CL] + k_{AP}^*K^1[CL]^n}{K^*(K^1 + [CL]) + K^1[CL]^n} \qquad (16)$$

and therefore the data of Figure 5 should be described by the following equation

$$\frac{k_{AP}}{k_{AP}^0} = \frac{K^1K^* + Y^1K^*[CL] + Y^*K^1[CL]^n}{K^*(K^1 + [CL]) + K^1[CL]^n} \qquad (17)$$

where Y^1 and Y^* denote the ratios k_{AP}^1/k_{AP}^0 and k_{AP}^*/k_{AP}^0, respectively, and the cardiolipin concentration is evaluated with respect to the apolar volume ($[CL] = [CL]_{apolar}$). Actually, eq 17 describes the experimental data well (see fit in Figure 5). The best fit parameters are $Y^1 = 1.06 \pm 0.02$, $Y^* = 6 \pm 2$, $n = 4 \pm 1$, $K^1 = 4 \pm 3$ mM, and $K_0 = (K^*)^{1/n} = 0.46 \pm 0.07$ M.

4. Discussion

According to the results of section 3.1, the binding affinity of the quinone for the Q_A site of the RC embedded in vesicles made of lecithin and cardiolipin is the same. This evidence rules out changes in the number of hydrogen bonds between the quinone molecule and the protein environment. Moreover, drastic changes in the protein−quinone mutual orientation are unlikely because a relevant variation in the strength of quinone−protein interactions is expected in such a case.

The rate of charge recombination from $P^+Q_A^-$ is essentially the same in the case of RC in detergent micelles (made of DDAO or OG) and lecithin vesicles. On the contrary, in the presence of cardiolipin, the light-induced $P^+Q_A^-$ state recombines faster (section 3.2). Such an effect is clearly discernible in different self-assembled amphiphile aggregates, namely, micelles and vesicles (Figures 3−5). A similar effect was qualitatively described (for RCs in DDAO micelles) in a recent paper by Rinyu et al.,[16] but the lack of quantitative data precludes a direct comparison. Instead, in that paper, detailed measurements on the yield of delayed fluorescence emission from the primary donor accompanying the $P^+Q_A^-$ charge recombination and on the rate of $P^+Q_AQ_B^-$ charge recombination are reported. The authors found, upon cardiolipin loading,

significant slowing of the charge recombination from $P^+Q_AQ_B^-$ that is accounted for by a 30 meV increase in the free energy drop from $P^+Q_A^-Q_B$ to $P^+Q_AQ_B^-$. Furthermore, on the basis of fluorescence measurements, they deduce a consistent decrease in the free energy drop from P^*Q_A to $P^+Q_A^-$.

As a whole, the results by Rinyu et al. suggest that cardiolipin induces an increase in the free energy level of the $P^+Q_A^-$ with respect to the neutral state of the RC.

In the high-temperature limit, electron transfer theories are well approximated by the celebrated Marcus expression[51]

$$k = \frac{2\pi}{\hbar} V^2 \frac{1}{\sqrt{4\pi\lambda KT}} \exp\left[-\frac{(\epsilon - \lambda)^2}{4\lambda KT}\right] \qquad (18)$$

that describes the dependence of the electron-transfer rate constant k on the driving force ϵ, the reorganization energy λ, and the electron coupling matrix element between initial and final states V (other symbols in eq 18 have their usual meaning). At room temperature, the effect of cardiolipin can be easily handled on the basis of the Marcus model by assuming that, upon CL loading, the driving force for $P^+Q_A^- \rightarrow PQ_A$ electron transfer increases (ϵ becomes more negative) leaving essentially unchanged V and λ values. Under these conditions, the ratio between the rate constants in the presence (k_{AP}) and in the absence (k_{AP}^0) of cardiolipin is

$$\frac{k_{AP}}{k_{AP}^0} = \exp\left[\frac{-(\epsilon^{CL} - \lambda)^2 + (\epsilon^\circ - \lambda)^2}{4\lambda KT}\right] \qquad (19)$$

where ϵ^{CL} and ϵ° are the driving forces for charge recombination in the presence and absence of cardiolipin, respectively. For RCs from *Rb. sphaeroides*, the value of ϵ° is estimated to be 0.52 eV,[52] and as above-discussed since the bound CL induces only a moderate change in the driving force of charge recombination ($\Delta\epsilon = \epsilon^{CL} - \epsilon^\circ = -30$ meV), one can rewrite eq 19 as

$$\frac{k_{AP}}{k_{AP}^0} \approx \exp\left[\frac{-2\Delta\epsilon(\epsilon^\circ - \lambda)}{4\lambda KT}\right] \qquad (20)$$

The value of reorganization energy for the $P^+Q_A^-$ recombination has been afforded in several investigations by varying the driving force (via substitution of the native ubiquinone with other type of quinones[53] or through site-directed mutants[54]) and/or by varying the temperature.[41,45,55] The resulting estimates for λ reveal a spread of values, ranging from 0.667 eV (ref 41) to 0.93 eV (ref 45). However, such a distribution of λ values has little effect on the outcome of the above equation because λ appears in both the numerator and denominator of the exponential argument. Indeed, the ratio k_{AP}/k_{AP}^0 evaluated according to eq 20 ranges from 1.15 to 1.30 in remarkable agreement with the independent experimental results summarized in Figure 5. It seems, therefore, that the peculiar dependence of the rate of $P^+Q_A^-$ recombination upon CL binding could be mainly ascribed to the increase, induced by cardiolipin, in the free energy drop associated to the $P^+Q_A^- \rightarrow PQ_A$ electron transfer (previously inferred from fluorescence experiments).[16] The interpretation on molecular terms is, however, delicate. Cardiolipin is a unique dianionic phospholipid with four acyl chains that could exert its effect directly on the electron acceptor or indirectly via specific (and presently unknown) lipid−protein interactions.

Following light absorption, the sudden appearance of separated charges inside the RC is an abrupt perturbation of its dark-adapted equilibrium state and adjustment of protein conformation begins immediately to accommodate the de novo charges of P^+ and Q_A^-. In RCs depleted of Q_B, the reduction of Q_A was observed to lead to rapid relaxation of the protein in a process that was suggested to involve several conformational substates. The relaxation, which at 300 K was calculated to occur in 1 ps to a few milliseconds, was explained by a decrease in both the driving force ϵ and the electronic coupling between acceptor and donor states V.[41] The RC relaxation from dark-adapted to light-adapted conformation is progressively hindered upon cooling, thus accounting for the striking increase in k_{AP}.[41,56] Parallel studies (reviewed in ref 57) performed *at room temperature* by embedding the protein within a solid sugar matrix fully confirm such a description of the interplay between protein dynamics and electron-transfer rate. On this basis, the increase in the free energy drop associated to the $P^+Q_A^- \rightarrow PQ_A$ electron transfer could reflect the hampering of relevant conformational motion. Two additional evidences support this point of view. First, the same increase in k_{AP} was found, in the absence of CL, in liquid solutions of trehalose where the internal dynamics of the RC is moderately slowed.[42] Second, it was previously demonstrated that the addition of cardiolipin improves the thermal stability of the RC,[18] evidence that suggests some CL-induced hampering of the unfolding dynamics.

The functional study here presented points to the existence of more than one site of binding for CL on the RC (see Figure 5), at difference with the unique site observed in the X-ray structures. The cardiolipin observed in RC crystals is tightly bound, as inferred from its presence in the RC embedded in lipidic cubic phases[20] (where the bicontinuous apolar domain furnishes a large solvent pool for CL). We expect, therefore, that a large fraction of our RCs retain that endogenous cardiolipin molecule. One can speculate that the high-affinity binding site ($K^1 = 4$ mM) seen in the CL titration of the RC (Figure 5) corresponds to a tightly bound cardiolipin molecule seen in several RC structures. According to such a hypothesis, the very small increase on k_{AP} could be explained by a limited effect due to the partial occupancy of the site by endogenous cardiolipin. At variance, the following features of the second class of binding sites permit the exclusion of any relation with the CL pocket recognized in X-ray structures:

(1) It is clearly a low-affinity binding. A *local* concentration of cardiolipin of about 0.5 M only slightly saturates the reaction center. For RC 1 μM, this corresponds to an *overall* CL concentration of about 100 μM that is close to the maximal loading of CL in aqueous DDAO solutions. Furthermore, the CL binding appears to be incomplete also in pure CL vesicles, thus we can certainly exclude that in RC crystals (without addition of exogenous CL) such sites are occupied.

(2) The binding of cardiolipin is clearly cooperative. This means that several CL molecules bind the RC. A rough estimate of the number of ligands involved in cooperative binding is given by the Hill coefficient (n in eq 11). According to the data of Figure 5, the RC accommodates about four molecules of cardiolipin, while in the RC structures only one CL molecule is observed.

Presently, we have indications neither on the location of these low-affinity binding sites nor on the mechanism of CL-induced destabilization of the $P^+Q_A^-$ state. The effect is, however, specific for cardiolipin and is not shared by lecithin.

A cooperative binding involves some conformational changes of the protein. The fit of the titration curve of Figure 5 to eq 17 gives $Y^* = 6 \pm 2$, and this correponds to a rate constant of $P^+Q_A^-$ recombination for the RC fully satured with CL equal

to $k_{AP}^* = 50 \pm 20\ s^{-1}$. This is close to the rate constant for P^+QA^- decay found at room temperature for the RC entrapped in a very rigid trehalose matrix ($k_{AP} = 35\ s^{-1}$), where conformational relaxation is severely inhibited.[57,58] This is consistent with the hypothesis that cardiolipin exerts its effect by hindering protein conformational motions.

Conclusions

In recent years, numerous structural studies have demonstrated that one molecule of cardiolipin tightly binds the photosynthetic reaction center from *Rb. sphaeroides*. The cardiolipin binding site seems to be highly preserved over the photosynthetic bacteria. In the present functional study, we showed that the addition of cardiolipin does not affect the affinity of the Q_A site for ubiquinone but has a relevant influence on the rate of $P^+Q_A^-$ recombination. The rate constant for the $P^+Q_A^- \rightarrow PQ_A$ electron transfer obtained in micelles and vesicles containing CL follows the same trend when cardiolipin concentration evaluated with respect to the apolar phase is used as a relevant variable. Moreover, our results reveal that there are two class of binding sites for cardiolipin. The high-affinity site is compatible with the binding site observed in crystallographic studies. On the contrary, the cooperative binding, involving about four CL molecules and taking place at high cardiolipin loading, is a feature previously unreported. It appears that the main effect of cardiolipin on the electron transfer can be ascribed to a destabilization of the charge-separated state. On the basis of previous studies, we propose that such an effect is likely due to CL-induced inhibition of protein conformational relaxation that stabilizes the light-induced $P^+Q_A^-$ state.

Acknowledgment. Financial support of MIUR of Italy is acknowledged by G.P., A.M., and Mauro G. (Grant PRIN/2003 "Nuovi biosensori basati su neurorecettori immobilizzati"). G.P., M.G., and M.G. were partially supported by the Consorzio Interuniversitario per lo sviluppo dei Sistemi a Grande Interfase (CSGI-Firenze). The authors thank Mr. G. Gervasoni for the technical support in building the sample compartment of the laser-photolysis apparatus.

Appendix: P^+ Decay in the Case of Slow CL Exchange

We start by assuming the rates of binding and release of cardiolipin to the RC−lipid complexes of scheme 9 are slow compared to the rate of charge recombination. Under this condition, each light-induced species undergoes independently exponential charge recombination

$$\frac{[P^+]_t}{[P^+]_{t=0}} = F^\circ \exp(-k_{AP}{}^0 t) + F^1 \exp(-k_{AP}{}^1 t) + F^* \exp(-k_{AP}{}^* t) \quad \text{(A1)}$$

where the fractions

$$F^\circ = \frac{[P^+Q_A{}^-]_t}{[P^+]_{t=0}} = \frac{[PQ_A]}{[RC]_{tot}}$$

$$F^1 = \frac{[P^+Q_A{}^-\cdot CL]_t}{[P^+]_{t=0}} = \frac{[PQ_A\cdot CL]}{[RC]_{tot}}$$

$$F^1 = \frac{[P^+Q_A{}^-\cdot (CL)_n]_t}{[P^+]_{t=0}} = \frac{[PQ_A\cdot (CL)_n]}{[RC]_{tot}} \quad \text{(A2)}$$

reflect the following dissociation equilibria *before* the saturating flash

$$R^1 = \frac{[PQ_A][CL]}{[PQ_A\cdot CL]}$$

$$R^* = \frac{[PQ_A][CL]^n}{[PQ_A\cdot (CL)_n]} \quad \text{(A3)}$$

and can be expressed as a function of the dissociation constant R^1 and R^* and of the cardiolipin concentration according to

$$F^\circ = \frac{1}{1 + \frac{[CL]}{R^1} + \frac{[CL]^n}{R^*}}$$

$$F^1 = \frac{[CL]}{R^1} \frac{1}{1 + \frac{[CL]}{R^1} + \frac{[CL]^n}{R^*}}$$

$$F^* = \frac{[CL]^n}{R^*} \frac{1}{1 + \frac{[CL]}{R^1} + \frac{[CL]^n}{R^*}} \quad \text{(A4)}$$

The rate constants are expected to have similar values, and in the presence of experimental noise, a safe deconvolution of the P^+ time course into three exponentials, according to eq A1, is not feasible. Instead, one can describe the multiexponential behavior by a cumulant expansion obtaining (to the second order)[34]

$$\frac{[P^+]_t}{[P^+]_{t=0}} = \exp\left(-\langle k_{AP}\rangle t + \frac{\sigma^2}{2} t^2\right) \quad \text{(A5)}$$

where $\langle k_{AP}\rangle$ and σ^2 are the mean and the variance of the charge recombination rate

$$\langle k_{AP}\rangle = F^\circ k_{AP}{}^0 + F^1 k_{AP}{}^1 + F^* k_{AP}{}^* \quad \text{(A6)}$$

$$\sigma^2 = F^\circ(k_{AP}{}^0 - \langle k_{AP}\rangle)^2 + F^1(k_{AP}{}^1 - \langle k_{AP}\rangle)^2 + F^*(k_{AP}{}^* - \langle k_{AP}\rangle)^2 \quad \text{(A7)}$$

using eq A4 and dividing eq A6 by $k_{AP}{}^0$, one obtains

$$\frac{\langle k_{AP}\rangle}{k_{AP}{}^0} = \frac{1 + \frac{Y^1}{R^1}[CL] + \frac{Y^*}{R^*}[CL]^n}{1 + \frac{[CL]}{R^1} + \frac{[CL]^n}{R^*}} \quad \text{(A8)}$$

The above equation can be rearranged by multiplying and dividing the right-hand term by R^*R^1, thus obtaining

$$\frac{\langle k_{AP}\rangle}{k_{AP}{}^0} = \frac{R^1R^* + Y^1R^*[CL] + Y^*R^1[CL]^n}{R^1R^* + R^*[CL] + R^1[CL]^n} \quad \text{(A9)}$$

an expression that is formally equivalent to eq 17 in the main text. The only difference is the meaning of the dissociation constants in the above equation that refer to the dark equilibria (A3).

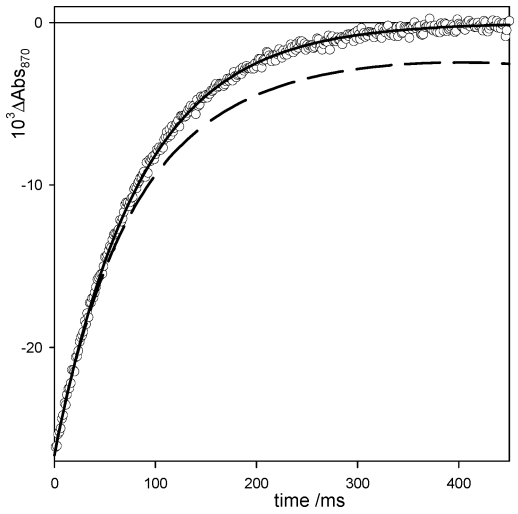

Figure 6. Time course of the absorbance change after a laser pulse for RC in DDAO micelles doped with CL (circles). Conditions: RC 2.3 μm, [CL]/[RC] = 103. The cardiolipin concentration in the apolar phase (eq 8) is $[CL]_{apolar} = 0.53$ M.

Note that for short times and small σ^2 values (i.e., $\sigma/\langle k_{AP}\rangle < 1$ and $\sigma t < 1$), eq A5 is approximately monoexponential with a decay constant $\approx\langle k_{AP}\rangle$. This point and the equivalence of eqs 17 and A9 indicate that the results of Figure 5 in the main text do not permit discrimination between fast and slow CL exchange. However, the features of the registered charge recombination kinetics are inconsistent with the hypothesis of slow cardiolipin exchange as detailed in the following.

According to eqs A6 and A7, the dependence of $\langle k_{AP}\rangle$ and σ on CL concentration are correlated. In particular, according to eqs A4, A6, and A7, the ratio $\sigma/\langle k_{AP}\rangle$ is expected to increase upon CL loading. The experimental charge recombination kinetics, however, do not follow such a prediction. A typical result is shown in Figure 6. The experimental trace (circles) recorded for the RC in DDAO micelles (RC 2.3 μM) doped with cardiolipin ([CL]/[RC] = 103 corresponding to $[CL]_{apolar} = 0.53$ M) is compared with the predictions for fast and slow CL exchange. For fast exchange, a single exponential with k_{AP} given by eq 17 is expected (solid line). On the contrary, in the case of slow exchange, the P^+ decay is expected to follow eq A5 with $\langle k_{AP}\rangle$ and σ given by eqs A9 and A7, respectively (dashed line). At short times, the two predictions coincide because eqs 17 and A9 are indistinguishable. However, at this high cardiolipin loading, eqs A6 and A7 foretell $\sigma/\langle k_{AP}\rangle = 0.46$, resulting in a clear deviation from the experimental data.

References and Notes

(1) Pauling, L.; Itano, H. A.; Singer, S.; Wells, I. C. *Science* **1949**, *110*, 543.

(2) Caffrey, M. *J. Struct. Biol.* **2003**, *142*, 108.

(3) Michel, H. *J. Mol. Biol.* **1982**, *158*, 567. Deisenhofer, J.; Epp, O.; Miki, K.; Huber, R.; Michel, H. *Nature* **1985** *318*, 618.

(4) Allen, J. P.; Feher, G.; Yeates, T. O.; Komiya, H.; Rees, D. C. *Proc. Natl. Acad. Sci. U.S.A.* **1987**, *84*, 5730.

(5) Gunner, M. R. *Curr. Top. Bioenerg.* **1991**, *16*, 319.

(6) Feher, G.; Allen, J. P.; Okamura, M. Y.; Rees, D. C. *Nature* **1989**, *33*, 111.

(7) McPherson, P. H.; Okamura, M. Y.; Feher, G. *Biochim. Biophys. Acta* **1990**, *1016*, 289.

(8) Shinkarev, V. P.; Wraight, C. A. In *The Photosynthetic Reaction Center*; Deisenhofer, J., Norris, J. R., Eds.; Academic Press: New York, 1993; Vol. 1, p 193.

(9) Fyfe, P. K.; Jones, M. R. *Biochim. Biophys. Acta* **2000**, *1459*, 413.

(10) Camara-Artigas, A.; Allen, J. P. *Photosynth. Res.* **2004**, *81*, 227.

(11) McAuley, K.; Fyfe, P. K.; Ridge, J. P.; Isaacs, N. W.; Cogdell, R. J.; Jones, M. R. *Proc. Natl. Acad. Sci. U.S.A.* **1999**, *96*, 14706.

(12) Jones, M. R.; Fyfe, P. K.; Roszak, A. W.; Isaacs, N. W.; Cogdell, R. J. *Biochim. Biophys. Acta* **2002**, *1565*, 206.

(13) Camara-Artigas, A.; Brune, B.; Allen, J. P. *Proc. Natl. Acad. Sci. USA* **2002**, *99*, 11055.

(14) Lee, A. G. *Biochim. Biophys. Acta* **2004**, *1666*, 62 and references therein.

(15) Dowhan, W. *Annu. Rev. Biochem.* **1997**, *66*, 199 and references therein.

(16) Rinyu, L.; Martin, E.; Takahashi, E.; Maroti, P.; Wraight, C. *Biochim. Biophys. Acta* **2004**, *1655*, 93.

(17) Nagy, L.; Milano, F.; Dorogi, M.; Agostano, A.; Laczko, G.; Szebenyi, K.; Varo, G.; Trotta, M.; Maroti, P. *Biochemistry* **2004**, *43*, 12913.

(18) Fyfe, P. K.; Isaacs, N. W.; Cogdell, R. J.; Jones, M. R. *Biochim. Biophys. Acta* **2004**, *1608*, 11.

(19) McAuley, K. E.; Fyfe, P. K.; Codgel, R. J.; Isaacs, N. W.; Jones, M. R. *FEBS Lett.* **2000**, *467*, 285.

(20) Katona, G.; Andréasson, U.; Landau, E. M.; Andréasson, L. E.; Neutze, R. *J. Mol. Biol.* **2003**, *331*, 681.

(21) Wakeham, M. C.; Sessions, R. B.; Jones, M. R.; Fyfe, P. K. *Biophys. J.* **2001**, *80*, 1395.

(22) Gray, K. A.; Wachtveitl, J.; Breton, J.; Oestherhelt, D. *EMBO J.* **1990**, *9*, 2061.

(23) Okamura, M. Y.; Isaacson, R. A.; Feher, G. *Proc. Natl. Acad.. Sci. U.S.A.* **1975**, *72*, 3491.

(24) Venturoli, G.; Mallardi, A.; Mathis, P. *Biochemistry* **1993**, *32*, 13245.

(25) Ambrosone, L.; Mallardi, A.; Palazzo, G.; Venturoli, G. *Phys. Chem. Chem. Phys.* **2002**, *4*, 3071.

(26) Nelder, J. A.; Mead, R. *Comput. J.* **1965**, *7*, 308.

(27) Press, W. H.; Flannery, B. P.; Teulkolsky, S. A.; Vetterling, W. T. *Numerical Recipes*; Cambridge University Press: Cambridge, U.K., 1986 and references therein.

(28) Mallardi, A.; Giustini, M.; Palazzo, G. *J. Phys. Chem. B* **1998**, *102*, 9168.

(29) Angelico, R.; Ceglie, A.; Olsson, U.; Palazzo, G. *Langmuir* **2000**, *16*, 2124.

(30) Milioto, S.; Romancini, D.; De Lisi, R. *J. Solution Chem.* **1987**, *16*, 943.

(31) Mallardi, A.; Palazzo, G.; Venturoli, G. *J. Phys. Chem. B* **1997**, *101*, 7850.

(32) McComb, J. C.; Stein, R. R.; Wraight, C. A. *Biochim. Biophys. Acta* **1990**, *1015*, 156.

(33) This is equivalent to expanding the ΔAbs(0) in the Taylor series around the mean local concentration of RC and quinone and retaining only the first term.

(34) Palazzo, G.; Mallardi, A.; Giustini, M.; Berti, D.; Venturoli, G. *Biophys. J.* **2000**, *79*, 1171.

(35) One cannot simply add ubiquinone as ethanol or DMSO solution because a *quantitative* transfer into the vesicle's bilayer cannot be assumed.

(36) In reverse micelles, the binding is complete already at a quinone concentration equal to 1 mM. In a typical proteoliposome preparation, this local concentration corresponds to a few quinone molecules per RC molecule.

(37) Beechem, J. M. *Methods Enzymol.* **1992**, *20*, 37.

(38) Straume, M.; Johnson, M. L. *Methods Enzymol.* **1992**, *210*, 117 and references therein.

(39) Correia, J. J.; Chaires, J. B. *Methods Enzymol.* **1994**, *240*, 593 and references therein.

(40) Krug, R. R.; Hunter, W. G.; Grieger, R. A. *J. Phys. Chem.* **1976**, *80*, 2335. Krug, R. R.; Hunter, W. G.; Grieger, R. A. *J. Phys. Chem.* **1976**, *80*, 2341. Krug, R. R.; Hunter, W. G.; Grieger, R. A. *Nature* **1976**, *261*, 566.

(41) McMahon, B. H.; Müller, J. D.; Wraight, C. A.; Nienhaus, G. U. *Biophys. J.* **1998**, *74*, 2567.

(42) Palazzo, G.; Mallardi, A.; Hochkoeppler, A.; Cordone, L.; Venturoli, G. *Biophys. J.* **2002**, *82*, 558.

(43) Hsi, E. S. P.; Bolton, J. R. *Biochim. Biophys. Acta* **1974**, *347*, 126.

(44) Hales, B. J. *Biophys. J.* **1976**, *14*, 471.

(45) Ortega, J. M.; Mathis, P.; Williams, J. C.; Allen, J. P. *Biochemistry* **1996**, *35*, 3354.

(46) Feher, G.; Okamura, M. Y.; Kleinfeld, D. In *Protein structure: Molecular and Electronic Reactivity*; Austin, R., Buhks, E., Chance, B., De Vault, D., Dutton, P. L., Fraunfelder, H., Goldanskii, V. I., Eds.; Springer-Verlag: New York, 1987; p 399.

(47) Francia, F.; Dezi, M.; Rebecchi, A.; Mallardi, A.; Palazzo, G.; Melandri, B. A.; Venturoli, G. *Biochemistry* **2004**, *43*, 14199.

(48) Hu, X.; Damianovic, A.; Ritz, T.; Schulten, K. *Proc. Natl. Acad. Sci. U.S.A.* **1998**, *95*, 5935. Walz, T.; Jamieson, S. J.; Bowers, C. M.; Bullough, P. A.; Hunter, C. N. *J. Mol. Biol.* **1998**, *282*, 833.

(49) Feher, G.; Okamura, M. Y. In *The Photosynthetic Bacteria*; Clayton, R. K., Sistrom, W. R., Eds.; Plenum Press: New York, 1978; p 349. Gast, P.; Hemerlijk, P.; Hoff, A. J. *FEBS Lett.* **1994**, *337*, 39.

(50) Robinson, N. C.; Zborowski, J.; Talbert, L. H. *Biochemistry* **1990**, *29*, 8962.
(51) Marcus, R. A.; Sutin, N. *Biochim. Biophys. Acta* **1985**, *811*, 265.
(52) Arata, H.; Parson, W. W. *Biochim. Biophys. Acta* **1981**, *638*, 201.
(53) Gunner, M. R.; Robertson, D. E.; Dutton, P. L. *J. Phys. Chem.* **1986**, *90*, 3783.
(54) Lin, X.; Murchison, H. A.; Nagarajan, V.; Parson, W. W.; Allen, J. P.; Williams, J. C. *Proc. Natl. Acad. Sci. U.S.A.* **1994**, *91*, 10265.
(55) Allen, J. P.; Williams, J. C.; Graige, M. S.; Paddock, M. L.; Labahn, A.; Feher, G.; Okamura, M. Y. *Photosynth. Res.* **1998**, *55*, 227.
(56) Kriegl, J. M.; Nienhaus, G. U. *Proc. Natl. Acad.. Sci. U.S.A.* **2004**, *101*, 123.
(57) Cordone, L.; Cottone, G.; Giuffrida, S.; Palazzo, G.; Venturoli, G.; Viappiani, C. *Biochim. Biophys. Acta* **2005**, *1749*, 252.
(58) Francia, F.; Palazzo, G.; Mallardi, A.; Cordone, L.; Venturoli, G. *Biochim. Biophys. Acta* **2004**, *1658*, 50.